

# Modeling of Indirect Evaporative Air Cooler for Thermal Performance Study

Guntars Fridenbergs<sup>1</sup>, Arturs Lesinskis<sup>2</sup>  
<sup>1-2</sup> Riga Technical University

**Abstract** – This paper presents a review, calculations and measurements based study on the parts of Indirect Evaporative Cooling (IEC) stand device, which have an influence on thermal performance. The study was undertaken considering a variety of aspects including background, history, current status, and concept. Parts of experimental stand device have been described as equations of heat and mass transfer in primary and secondary air and water flows. The model has been validated with self-made device measurements in the laboratory. The main goal has been to make a working stand device for future research of IEAC device cooling efficiency, which mostly depends on mass flow rates of primary and secondary air flows and spacing between the plates of wet and dry passages.

**Keywords** – IEAC stand device, indirect evaporative air cooler, cooling efficiency, heat and mass transfer

## I. INTRODUCTION

To determine the parameters, the experimental stand device was studied (Fig.1). Two main parameters discovered influencing on cooling performance are water consumption and water exchange cycle.

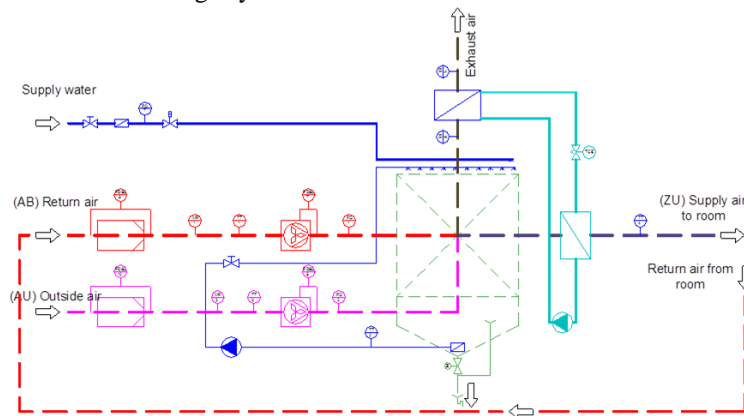


Fig.1. Practical model of the studied device [2].

1. Water consumption of evaporative air conditioners includes the water evaporated to provide the cooling effect.

2. Water exchange cycle is water dumped off in a predicted period of time for the purpose of cleaning and avoiding high salt concentration.

## II. WATER EVAPORATION

The psychrometric chart in Fig. 2 illustrates the evaporation process (blue line) when the air passes through the wet side of indirect evaporative air conditioner. At the given entry air conditions ( $t_1, t_1'$ ) and evaporation effectiveness ( $\mathcal{E}_e$ ), the dry-bulb temperature of the leaving air ( $t_2$ ) can be calculated

according to Eq. 1. In ideal conditions, the wet-bulb temperature of the leaving air is the same as the wet-bulb temperature of the entering air. Then the humidity ratios of both entering and leaving air can be determined from the psychrometric chart (Fig. 1). The water consumption rate for cooling purpose can be estimated using Eq. 2 [3,4,5].

$$t_2 = t_1 - \frac{\mathcal{E}_e}{100} \cdot (t_1 - t_1') \quad (1)$$

$$\dot{m}_e = \rho \dot{V} (w_2 - w_1) / 1000 \quad (2)$$

where  $\dot{m}_e$  – water consumption rate, kg/h;  $\dot{V}$  – air volumetric flow rate, m<sup>3</sup>/h;  $\rho$  – air density, 1.2041 kg/m<sup>3</sup>;  $w_1$ ,  $w_2$  – humidity ratios of entering and leaving air, g moisture/kg dry air.

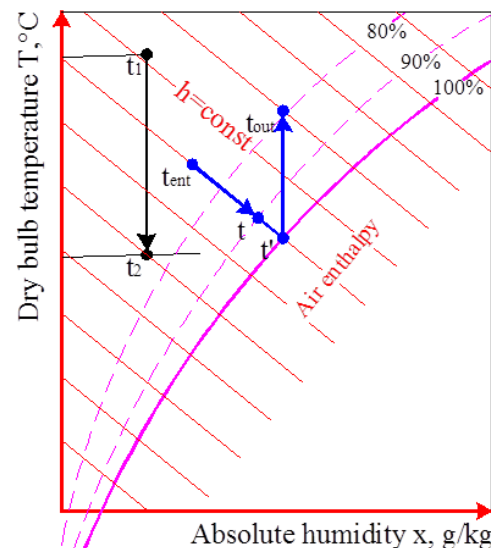


Fig.2. Psychrometrics of two-stage evaporative cooler [2].

The water consumption rate due to evaporation varies depending on the air flow rate, the temperature and humidity of the outside air and the pad characteristics. Some manufacturers quote indicative figures for water consumption but these can only be used as approximate values. In an effort to provide independent values of the water required for evaporation, the water consumption rates for cooling purposes can be calculated in different locations. The design temperature and humidity can be based on typical historical data and be used to represent the maximum cooling conditions.

### III. WATER EXCHANGE CYCLE

#### A. Modeled device

The cell element selected for numerical analyses (Fig.3.) is shown in Fig. 4. The element consists of half the height of the dry channel, the plate wall and half the height of the wet channel. Energy balance equations were applied to each single element, with consideration of a pre-set boundary condition. This allowed the temperature and humidity distribution across the dry and wet channel sections to be established.

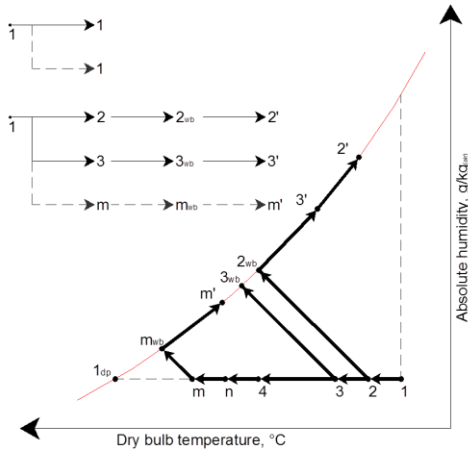


Fig.3. Selected IEAC cooler operation cycle in H-x diagramm [2].

To simplify the modelling process and mathematical analysis, the following assumptions were made:

1. The heat and mass transfer is in steady state. The IEAC enclosure is considered as the system boundary.
2. The wet surface of the fibre-sheet is completely saturated. The water vapour is distributed uniformly within the wet channel.

3. A temperature gradient for the channel cross-section was set to zero. Heat transfer in the separating plate is considered in the vertical direction only. Within the working fluid, the cross-stream convective heat transfer is considered as the dominant mechanism of heat transfer.

4. Each element has a uniform wall surface temperature. An analysis carried out by Zhao et al. showed that the thermal conductivity of the plate wall has a little impact on the magnitude of the heat and mass transfer rates, due to its small thickness (0.24 mm). The temperature difference between dry and wet sides of the wall can be ignored.

5. Air is treated as an incompressible gas.

The mass balance in the wet channel can be expressed by Eq. 3:

$$\left(\frac{m_{a,f2}}{2}\right) dw_{a,f2} = h_m (\rho_{w,a2} + \rho_{a,f2}) \quad (3)$$

where  $m_{a,f2}$  – air mass flow rate, kg/s;  $w_{a,f2}$  – humidity ratio of moist air, kg/kg dry air;  $h_m$  – mass transfer coefficient, m/s  
 $\rho$  – density, kg/m<sup>3</sup>

The general energy balance within the element in Fig. 4 can be expressed as Eq. 4:

$$dQ_1 = dQ_2 + dQ_3 \quad (4)$$

where  $Q$  – heat flux, W/m<sup>2</sup>

The energy balance in dry passages – dry passage air involves the forced convective heat transfer, leading to change of the enthalpy of the air. Energy balance in a dry passage could be written as Eq. 5:

$$dQ_1 = h_1 (t_{a,f1} + t_w) dA = \left(\frac{m_{a,f1}}{2}\right) di_{a,f1} \quad (5)$$

where  $A$  – heat transfer area, m<sup>2</sup>;  $i$  – specific enthalpy of air, J/kg

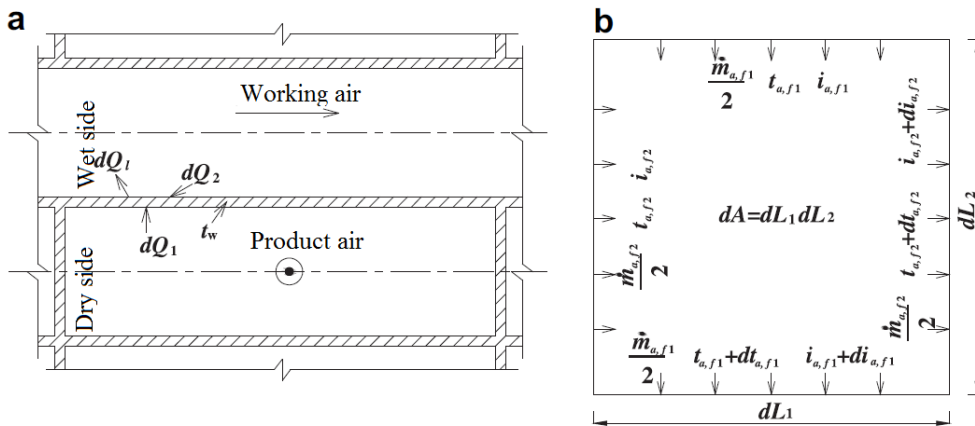


Fig.4. Cell element (a) applied for numerical simulation, differential illustration (b).

The energy balance in wet passages – wet passage air involves the forced heat and mass exchange, which leads to a change of enthalpy of the air within the passages. The energy balance within the passages can be written as Eq. (6):

$$dQ_1 - dQ_2 = \left(\frac{m_{a,f2}}{2}\right) dw_{a,f2} \quad (6)$$

where, for the forced convective heat and mass transfer occurring in the wet passages respective Eq. (7) and Eq. (8) can be written

$$dQ_2 = h_2 (t_{a,f2} + t_w) dA \quad (7)$$

$$dQ_1 = (\rho_{w,a2} + \rho_{a,f2}) \gamma dA \quad (8)$$

The air flow within the pipes remains in a laminar flow state when  $ReD < 2300$  and becomes turbulent flow when  $ReD > 4000$ . Due to the passage size and air velocity, the air flow within the passage is considered to be laminar. In this case, the thermal entry length for laminar flow can be calculated as follows (Eq. 9):

$$\frac{L}{d} = 0.05Re \cdot Pr \quad (11)$$

For both entry region and fully developed flow conditions, the Nusselt number can be calculated using the following equation (10):

$$Nu = 1.86 \left( \frac{Re \times Pr}{\frac{L}{d}} \right)^{1/3} \left( \frac{\eta_{a,f}}{\eta_{w,a}} \right)^{0.14} \quad (10)$$

The thermal entrance Nusselt numbers are higher than those for the fully developed case. For the developing flow conditions in the entry region, the Nusselt number can be calculated as presented below by Eq. (11):

$$Nu = 3.66 + \frac{0.0668 \cdot Re \cdot Pr \left( \frac{d}{L} \right)}{1 + 0.04 \left[ Re \cdot Pr \left( \frac{d}{L} \right) \right]^{2/3}} \quad (11)$$

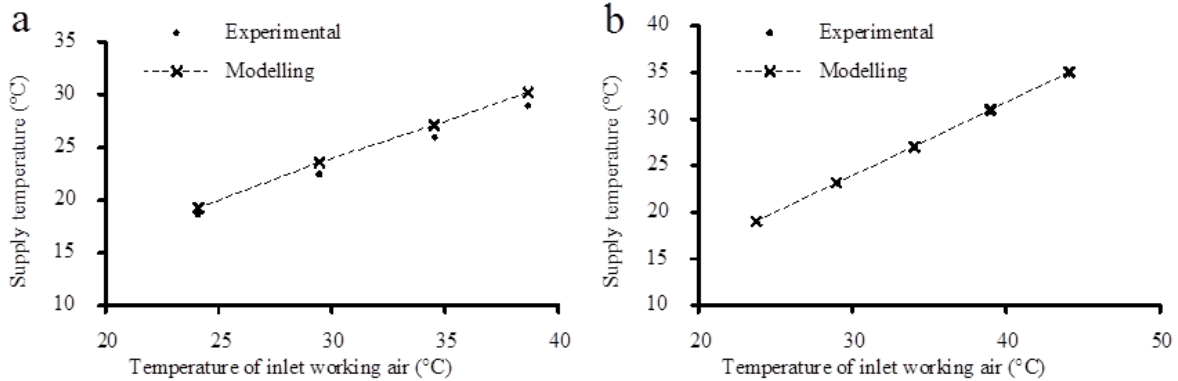


Fig.5. Experimental validation of supply air temperature. (a) Case 1. (b) Case 2

Case 1 and Case 2 were modelled at constant air flow rate 150 m<sup>3</sup>/h ( to compare with C. Zhan past calculations) and dry bulb 25 till 40 °C. In Case 1 RH=35%, in Case RH=50%, that is the main difference.

The mass transfer coefficient between wet passage air flow and the wet surface of the wall may be calculated using the following equation (12):

$$\frac{h}{h_m} = \rho c_p L e^{2/3} \quad (12)$$

The mathematical expression for wet-bulb effectiveness  $\varepsilon_{wb}$  can be written as follows (Eq. 13):

$$\varepsilon_{wb} = \frac{t_{db,wk,in} - t_{db,su}}{t_{db,wk,in} - t_{wb,wk,in}} \quad (13)$$

The theoretical energy efficiency coefficient of performance (COP) of the system can be defined as the ratio of cooling capacity and fan power consumption:

$$COP = \frac{\Phi_0}{P} \quad (14)$$

Cooling capacity ( $\Phi_0$ ) can be expressed as Eq. (15):

$$\Phi_0 = m_{pt} (i_{wk,in} - i_{wkpt,in}) \quad (15)$$

where  $m_{pt}$  - product air mass flow rate, kg/s;  $i_{wk,in}$  - specific enthalpy of inlet working air, J/kg;  $i_{pt}$  - product air enthalpy, J/kg

The theoretical fan power (P), can be written as Eq. (16):

$$P = \Delta p_{wk} V_{wk} + \Delta p_{pt} V_{pt} \quad (16)$$

where  $\Delta p_{wk}$  - working air pressure loss, Pa;  $V_{wk}$  - working air flow rate, m<sup>3</sup>/s;  $\Delta p_{pt}$  - product air pressure loss, Pa;  $V_{pt}$  - product air flow rate, m<sup>3</sup>/s.

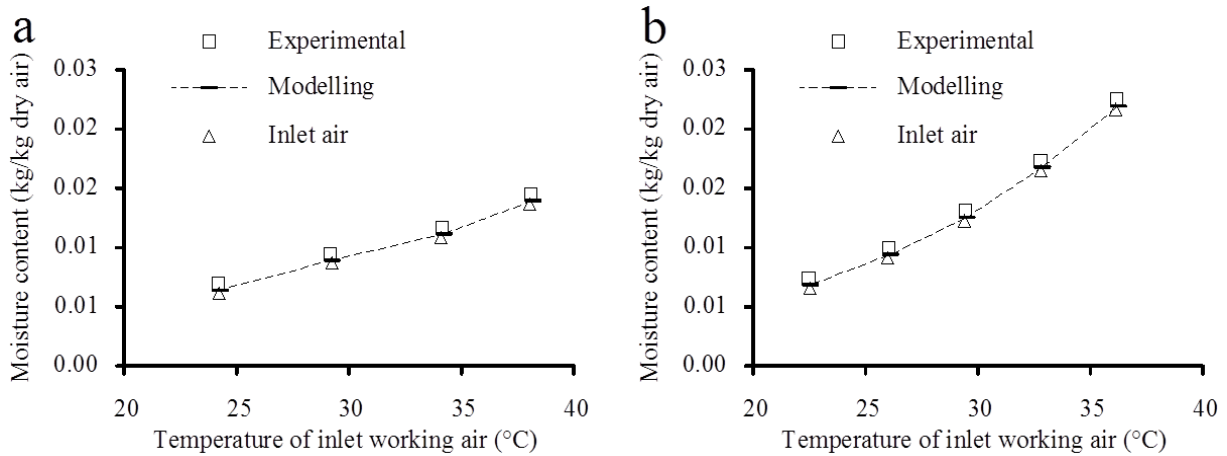


Fig.6. Experimental validation of supply air moisture content in Case 1 (a) and Case 2 (b).

It should be emphasized that the energy efficiency obtained from the simulation is an ideal value, which involves the use of the theoretical fan power. Actual fan power will be 120–170 % of the ideal value, leading to a drop in the calculated efficiency by 60–80 %. It should be noted that in this paper all the subsequent figures related to COP are ‘ideal’ rather than ‘practical’ values.

### B. Results

The result of the calculation is determined considering the temperature distribution of the heat exchanger plates, which

then will allow exploring the heat transfer across the heat exchanger volume, as well as allow for the calculation of geometrical effects on the final parameters.

The supply air temperature and the return air temperature just behind the first part of the heat exchanger were in good agreement with the measured data. The model underestimated the temperature of the exhaust air because it does not take into account the fact that the return air is heated by the recirculated water in the second part of the heat exchanger (Fig. 7.).

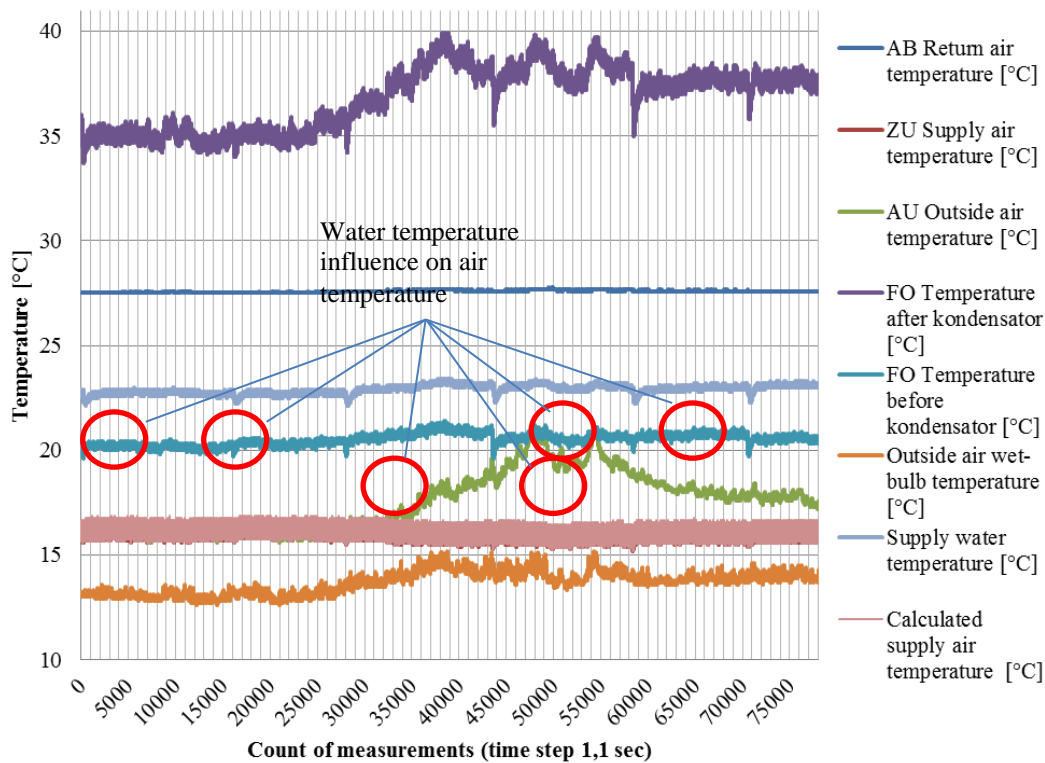


Fig.7. The observed and calculated water temperature fluctuations on IEAC heat exchanger.

#### IV. CONCLUSIONS

Comparing the two major components of water usage in evaporative air conditioners (water used for the cooling effect and water dumped/bled off), it may be concluded that if the water bleeding/dumping system is well designed, set and maintained, the total water consumption will be largely dominated by the moisture evaporation which is essential in operating the evaporative cooler. However, if not properly adjusted, the water bleeding/dumping rate is of the same order of magnitude as the evaporation rate and can lead to considerable wastage of valuable water.

An integrated simulation methodology of the building with its indirect evaporative cooling installation is necessary in order to take into account both heat and mass balance in building calculations. It is concluded that for future researches it is important to make calculations because of multiple available publications. In this way it is possible to study the interaction between the thermal performance of an indirect evaporative cooling system and the moisture balance of a room. The IEC-effectiveness was studied using measurements in an AHU containing an indirect evaporative cooling system.

A new aspect that has been found in literature is that the thermal effectiveness is independent of the inlet conditions of the outdoor and return air. It is important for future researches.

#### V. REFERENCES

- [1] CERCI Y. A new ideal evaporative freezing cycle. *International Journal of Heat and Mass Transfer* 2003 – p. 1–11.
- [2] CIBSE KNOWLEDGE SERIES: sustainable low energy cooling: an overview. Plymouth PL6 7PY, UK: Latimer Trend & Co. Ltd, 2005.;
- [3] COSTELLOE B, FINN D. Indirect evaporative cooling potential in air e water systems in temperate climates. *Energy and Buildings*, 2003.
- [4] FRĪDENBERGS, G., LEŠINSKIS, A., Evaluation of indirect evaporative cooler in public buildings, RTU, 2012 – p. 6–48.
- [5] HALASZ, B., A general mathematical model of evaporative cooling devices, *Rev. Gén. Therm., FR*, Vol. 37 – 1998. – p. 245–255.
- [6] HASAN A, SIREN K. Theoretical and computational analysis of closed wet cooling-towers and its applications in cooling of buildings. *Energy and Buildings - 2002* – p. 34.
- [7] KALS WA. Wet-surfaces air coolers, *Chemical Engineering* – 1971. – p. 68.
- [8] Latvijas Metroloģijas centra data base [referred on the 3th of January in 2012 y.]. [www.meteo.lv/pdf\\_base/meteor\\_2009.html](http://www.meteo.lv/pdf_base/meteor_2009.html).
- [9] MACLAINE-CROSS, I. L., BANKS, P. J., A general theory of wet surface heat exchangers and its application to regenerative evaporative cooling, *Journal of Heat Transfer*, Vol.103, No. 3, - 1981. – p. 579–585.
- [10] MCCLELLAN, C. H., Estimated temperature performance for evaporative cooling systems in five locations in the United States, *ASHRAE Transactions*, 94 (2), - 1988. – p. 1071–1090.
- [11] MIZUSHINA RIT, MIYASHITA H. Characteristics and methods of thermal design of evaporative coolers, *International Chemical Engineering* – 1968 – p. 3–8.
- [12] MIZUSHINA RIT, MIYASHITA H. Experimental study of an evaporative cooler, *International Chemical Engineering* 1967. – p. 4–7.
- [13] NIITSU Y, NAITO K, ANZAI T. Studies on characteristics and design procedure of evaporative coolers, *Journal of SHASE, Japan* – 1969. – No.7 – p. 12–23.
- [14] PARKER RO, TREYBAL RE. The heat-and-mass transfer characteristics of evaporative coolers, *Chemical Engineering Progress Symposium Series* – 1961 – p. 57.
- [15] PETERSON JL. An effectiveness model for indirect evaporative coolers, *ASHRAE Transactions* – 1993. – p. 99.
- [16] SETHI VP, SHARMA SK. Survey of cooling technologies for worldwide agricultural greenhouse applications. *Solar Energy*, 2007.
- [17] STABAAT, P., MARCHIO, D, Simplified model for indirect-contact evaporative cooling-tower behaviour, *Applied Energy* 78 (2004), - 2003 – p. 433–451.
- [18] SCHIBUOLA, L., High-efficiency recovery for air-conditioning applications in a mild climate: a case study, *Applied Thermal Engineering*, Vol. 17, No. 5 – 1997. – p. 447–454.
- [19] Supple, R. G., Broughton, D. R., "Indirect evaporative cooling – Mechanical cooling design", *ASHRAE Transactions*, Vol. 91, Part 1B – 1985. – p. 319–328
- [20] ZHAO X, DUAN Z, ZHAN C, RIFFAT SB. Dynamic performance of a novel dew point air conditioning system for the UK climate. *International Journal of Low Carbon Technology* 2009.
- [21] Zhiyin D, Changhong Z, ZHAN C, RIFFAT SB. Indirect evaporative cooling: Past, present and future potentials, *Renewable and sustainable energy reviews* – 2012. - p. 1–28.